Available online at www.sciencedirect.com
ScienceDirect
Biochimica et Biophysica Acta 1767 (2007) 362–373
Biochimica et Biophysica Acta
BBA
www.elsevier.com/locate/bbabio

A pathway for protons in nitric oxide reductase from *Paracoccus denitrificans*

Joachim Reimann, Ulrika Flock, Håkan Lepp, Alf Honigmann [1], Pia Ädelroth *

Department of Biochemistry and Biophysics, The Arrhenius Laboratories for Natural Sciences, Stockholm University, SE-106 91 Stockholm, Sweden

Received 13 November 2006; received in revised form 28 February 2007; accepted 1 March 2007
Available online 16 March 2007

Abstract

Nitric oxide reductase (NOR) from *P. denitrificans* is a membrane-bound protein complex that catalyses the reduction of NO to N_2O ($2NO + 2e^- + 2H^+ \rightarrow N_2O + H_2O$) as part of the denitrification process. Even though NO reduction is a highly exergonic reaction, and NOR belongs to the superfamily of O_2-reducing, proton-pumping heme-copper oxidases (HCuOs), previous measurements have indicated that the reaction catalyzed by NOR is non-electrogenic, i.e. not contributing to the proton electrochemical gradient. Since electrons are provided by donors in the periplasm, this non-electrogenicity implies that the substrate protons are also taken up from the periplasm. Here, using direct measurements in liposome-reconstituted NOR during reduction of both NO and the alternative substrate O_2, we demonstrate that protons are indeed consumed from the 'outside'. First, multiple turnover reduction of O_2 resulted in an increase in pH on the outside of the NOR-vesicles. Second, comparison of electrical potential generation in NOR-liposomes during oxidation of the reduced enzyme by either NO or O_2 shows that the proton transfer signals are very similar for the two substrates proving the usefulness of O_2 as a model substrate for these studies. Last, optical measurements during single-turnover oxidation by O_2 show electron transfer coupled to proton uptake from outside the NOR-liposomes with a $\tau = 15$ ms, similar to results obtained for net proton uptake in solubilised NOR [U. Flock, N.J. Watmough, P. Ädelroth, Electron/proton coupling in bacterial nitric oxide reductase during reduction of oxygen, Biochemistry 44 (2005) 10711–10719]. NOR must thus contain a proton transfer pathway leading from the periplasmic surface into the active site. Using homology modeling with the structures of HCuOs as templates, we constructed a 3D model of the NorB catalytic subunit from *P. denitrificans* in order to search for such a pathway. A plausible pathway, consisting of conserved protonatable residues, is suggested.

Keywords: Proton transfer; Electron transfer; Proteoliposomes; Flow-flash; Non-heme iron; Nitric oxide; Oxygen; Homology modeling; Sequence alignments

1. Introduction

Bacterial denitrification is a process in which nitrate is stepwise reduced via nitrite, nitric oxide and nitrous oxide to dinitrogen, which is released into the atmosphere. The reduction of NO to N_2O (see Eq. (1)) is catalyzed by nitric oxide reductase (for reviews, see [1,2]).

$$2NO + 2H^+ + 2e^- \rightarrow N_2O + H_2O \quad (1)$$

Bacterial nitric oxide reductases (NOR) are integral membrane proteins, and homology searches for the large catalytic subunit (NorB) showed that NOR is a divergent member of the superfamily of O_2-reducing heme-copper oxidases (HCuOs). The HCuOs are characterized by having a large catalytic subunit with six invariant histidines at the same positions in 12 (predicted for NOR) transmembrane helices [3,4]. In the HCuOs, for which crystal structures are known both for the mitochondrial enzyme [5] and for several bacterial enzymes [6–9], these histidines coordinate two heme groups and a copper ion.

Abbreviations: NOR, bacterial nitric oxide reductase; HCuO, heme-copper oxidase; C*c*O, cytochrome *c* oxidase; DDM, β-D-dodecyl maltoside; HEPES, 4-(2-Hydroxyethyl)-piperazine-1-ethanesulfonic acid; BTP, Bis-Tris Propane; HARC, hexa-ammineruthenium(II)-chloride; v-NOR, NOR reconstituted into lipid vesicles; s-NOR, detergent solubilised NOR; FCCP, carbonyl cyanide-*p*-trifluoromethoxyphenyl-hydrazon; MSA, multiple sequence alignments; rmsd, root mean square deviation; Aas, amino acids

* Corresponding author. Tel.: +46 8 164183; fax: +46 8 153679.
E-mail address: piaa@dbb.su.se (P. Ädelroth).
[1] Current address: Biophysik, Universität Osnabrück, FB Biologie/Chemie, D-49034 Osnabrück, Germany.

0005-2728/$ - see front matter © 2007 Elsevier B.V. All rights reserved.
doi:10.1016/j.bbabio.2007.03.006

In the NORs, for which there is no structural information at atomic detail, in analogy with the HCuOs, two of the conserved histidines coordinate a low-spin heme and one coordinates a high-spin heme. The remaining three histidines, which in the HCuOs coordinate the copper ion, presumably coordinate a non-heme iron in NOR [10,11].

The large subunit of the NORs can be divided into two subclasses, called NorB and NorZ, with high similarity, but with the difference that the NorZ contains a ~300 amino acid extension at the N-terminal, which is why these two forms are also called short-chain (sc) and long-chain (lc) NORs. The NorB form is isolated in complex with another protein, the NorC, which contains a *c*-type cytochrome (cyt.) and receives electrons from water-soluble donors such as cyt. *c* [1]. The NorZ has been purified in a single subunit form that receives electrons from quinol [12], which has led to the two NOR classes also being termed cNOR (for cyt. *c*) and qNOR (for quinol).

The NOR from *Paracoccus* (*P.*) *denitrificans* is a cNOR, purified as a complex between NorB and NorC. NorB harbors a low-spin heme *b*, a high-spin heme b_3, and a non-heme iron, Fe_B. The heme b_3 and Fe_B form a binuclear center, which is the site of NO-reduction. NorC is a membrane-anchored protein harboring a low-spin heme *c*, which is believed to be the site of electron entry from the water-soluble electron donor, in *P. denitrificans* either cyt. c_{551} or pseudoazurin [1].

The HCuOs (for reviews see e.g. [13–16]) catalyze the four-electron reduction of oxygen to water (Eq. (2a)), and use the free energy available from this reaction to generate an electrochemical proton gradient across the membrane (Eq. (2a) and (2b)).

$$O_2 + 4H^+ + 4e^- \rightarrow 2H_2O \quad (2a)$$

$$4H^+_{in} \rightarrow 4H^+_{out} \quad (2b)$$

The *P. denitrificans* NOR can, in addition to the physiological NO-reduction, also catalyze the reduction of dioxygen (Eq. (2a)) to water [17–19]. The O_2- and NO-reduction activities are closely correlated, presumably because the same catalytic components are involved in both processes.

The HCuOs generate an electrical gradient by using electrons and protons derived from opposite sides of the membrane; the protons used for water formation (substrate protons, Eq. (2a)) are derived exclusively from the 'inside' (the mitochondrial matrix or bacterial cytoplasm) and the electrons from the 'outside', e.g. from periplasmic cyt. *c*. In addition, the HCuOs couple the electron transfer to oxygen (E'_0=+0.8 V) to the translocation of $4H^+/O_2$ through the protein (Eq. (2b)) across the membrane. In HCuOs with high sequence similarity to the mitochondrial oxidase (termed type A1 [15]), protons are transferred from the cytoplasmic surface of the protein into the active site through well-characterised pathways, called the D- and the K-pathway, consisting of protonatable residues and water molecules (for a review on proton transfer in proteins see [20]). The D-pathway is used for both substrate and pumped protons (6–7 in total) during the oxidative part of the catalytic cycle, whereas the K-pathway is probably used for (1–2) protons during the reductive part (see e.g. [21,22]). The D-pathway starts at the cytoplasmic surface with the Asp-132 (*R. sphaeroides* aa_3 numbering[2]). It then continues through a network of water molecules stabilised by polar residues up to the essential Glu-286, which sits at a ~10 Å distance from Cu_B.

In the NORs, these residues, shown in the A1 HCuOs to be crucial for proton transfer/pumping are not conserved (but see Discussion), and available data, from whole cell measurements [23,24] or using an electrometric technique [25] indicate that the two-electron reduction of NO catalyzed by NOR is non-electrogenic, i.e. not coupled to charge translocation across the membrane. This can seem surprising since the free energy available from reducing NO (E'_0=+1.2 V) is even larger than for O_2 reduction.

As electrons are supplied by soluble donors from the periplasmic side of the membrane, the lack of electrogenicity in NOR implies that not only is NOR not a proton pump, but also that the substrate protons needed for NO-reduction (see Eq. (1)) must come from the periplasm.

In order to study the mechanism of proton transfer in NOR, we have previously used O_2 as the oxidant since the chemical reactivity of NO in aqueous solutions hampers direct measurements of proton consumption using pH-sensitive dyes in unbuffered solutions. We thus characterized the single-turnover reaction between fully reduced detergent-solubilised NOR and O_2 using the flow-flash technique in combination with time-resolved optical measurements [19]. Our results showed that oxygen binds to heme b_3 with a τ=40 μs (at 1 mM O_2), after which electron transfer from the low-spin hemes *b* and *c* to the O_2 bound at the binuclear site occurs with a τ=25 ms (at pH 7.5). A slow phase of oxidation of hemes *b* and *c* with τ ~1 s presumably completes the reduction of O_2 to H_2O. The τ=25 ms (k=40 s^{-1}) phase is coupled to proton uptake from the bulk solution, and the rate constant shows a pH dependence consistent with limitation by internal proton transfer (with a k_{max}=250 s^{-1} at low pH) into the active site from a protonatable group. This group is in rapid equilibrium with the bulk solution, has a pK_a=6.6 and was suggested to be an amino acid located close to the active site [19,26].

In this work, the aim was to confirm or disprove, by direct measurements, the indication that in NOR, protons are supplied from the periplasmic space. Having established from which side of the membrane the protons originate, our aim was further to search for putative proton transfer pathways into the NOR active site. To this end, we reconstituted NOR into phospholipid vesicles, and studied proton consumption by the liposome-reconstituted NOR (v-NOR) in several different ways. First during several turnovers of O_2-reduction using a pH-sensitive dye added to the outside of the vesicles. Second, we studied the single-turnover oxidation of fully reduced v-NOR using the flow-flash technique in combination with electrometric detection in order to compare proton transfer characteristics with O_2 as the substrate to those using the physiological substrate NO. Third, we studied the same reaction between fully reduced

[2] Unless otherwise indicated, for the A1 HCuOs, numbering of residues will from here on be according to the *R. sphaeroides* aa_3 sequence.

v-NOR and O_2 but with optical detection using a pH-sensitive dye added to the outside of the vesicles. Taken together, the results from the different measurements show that O_2 is a good model for studying proton transfer in NOR, and that protons are consumed from the outside of the liposomes. Having established that protons are delivered to the active site from the outer surface of NOR, we constructed, by homology modeling using the X-ray structures for the conventional HCuOs, a three-dimensional model of the catalytic subunit NorB. The model was used in order to search for putative proton transfer pathways, presumably consisting of protonatable residues. From the model, and from a search for conserved protonatable residues, a proton transfer pathway as well as candidates for the previously identified proton donor to the catalytic site are suggested.

2. Materials and methods

2.1. Growth of bacteria and purification of NOR

The NOR used in this study was from *Paracoccus (P.) denitrificans*, expressed in *Escherichia (E.) coli* JM 109 using the expression system described in [18]. Growth of bacteria, preparation of membranes and purification of NOR was essentially as described in [18], with the same changes as described in [19]. After purification, NOR was rapidly frozen in N_2*(l)* and stored at −80 °C until needed.

2.2. Reconstitution of NOR into liposomes

Reconstitution of NOR into liposomes was achieved by the Bio-Beads method according to [27], which is modified from [28,29]. Briefly, detergent solubilized NOR was diluted to 4–6 μM in 100 mM HEPES, pH 7.4, and 4% (w/v) cholic acid. Lipid vesicles were formed by sonication of 40 mg/ml L-α-phosphatidylcholine (type II-S from soybean, Sigma) in 2% cholic acid and 100 mM HEPES, pH 7.4. Enzyme and liposomes were mixed 1:1 and detergent was removed by consecutive additions of Bio-Beads (Bio-Rad Laboratories) and a PD-10 column (Amersham Biosciences). This method results in proteoliposomes with a diameter of ~40 nm [27]. Proteoliposomes were kept cold and under N_2 and used on the same day.

The orientation of NOR in the liposomes, measured essentially as in [30], was ~90% 'right-side out', i.e. with the soluble part of NorC facing the outside solution.

For the measurements of proton uptake using the pH-sensitive dye phenol red, the samples used need a low buffering capacity and were thus passed over a PD-10 column equilibrated with the desired unbuffered solution (see below).

The O_2-reduction activity of NOR in liposomes was measured as in [19] and found to be ~10 $e^- s^{-1}$. NO stock solutions were prepared from NO gas (Aga) as in [10]. The NO-reduction activity was measured using a Clark electrode (Hansatech) with a variable voltage setting (polarized at −0.8 V) essentially as in [10] and found to be 40–60 $e^- s^{-1}$. Thus, the catalytic activity of NOR in vesicles was as high (or higher) as in the solubilized protein.

The 'respiratory control ratio' (RCR), i.e. the ratio of the catalytic activity in the absence and presence of the uncouplers FCCP (carbonyl cyanide-*p*-trifluoromethoxyphenyl-hydrazon) and valinomycin was found to be =1 for both NO and O_2 as electron-accepting substrates.

2.3. Stopped-flow measurements

In order to measure proton consumption by v-NOR during multiple turnovers with O_2, a stopped-flow apparatus (Applied Photophysics) was used. To start the reaction 0.2 μM v-NOR in 45 mM KCl, 45 mM sucrose, 0.5 mM EDTA, pH ~7.6 were mixed in a 1:1 ratio with 10 μM reduced cyt. *c* in 45 mM KCl, 45 mM sucrose, 0.5 mM EDTA, 100 μM phenol red, pH ~7.6. For studying changes in phenol red absorbance, λ = 559 nm was chosen since it was found (in separate experiments, data not shown) to be the isobestic point for cyt. *c* oxidation, which was studied at 550 nm. In a second set of measurements, 20 μM of the protonophore FCCP and 10 μM of the K^+ ionophore valinomycin were added to v-NOR before mixing in order to dissipate any forming electrochemical proton gradient. The same experiment was also repeated in the presence of 10 mM HEPES (pH 7.6) in order to confirm that changes in absorbance at 559 nm were indeed due only to proton consumption by v-NOR.

In order to relate the observed changes in absorbance at 559 nm to the change in proton concentration, the exhaust from the stopped-flow apparatus was placed in a cuvette under N_2 and adjusted (if necessary) to pH ~7.6. Subsequently, the buffering capacity of the solution ($\Delta A^{559}/\Delta[H^+]$) was measured by adding known amounts of HCl and recording the changes in absorbance at 559 nm.

Cyt. *c* was reduced with hydrogen gas using Platinum black as a catalyst [31].

2.4. Electrometric measurements

The set-up for measuring voltage changes is of local design (details to be described elsewhere (Lepp et al., manuscript in preparation)), based on the method developed originally by Drachev et al. [32] and modified for use with the flow-flash technique by Verkhovsky et al. [33]. Briefly, Ag/AgCl electrodes record the voltage between two compartments that are separated by a thin lipid-impregnated Teflon film. Liposomes containing NOR are attached to one side of the Teflon film by incubation in 20 mM CaCl. The voltage across the Teflon film is proportional to the potential across the vesicle membranes, making it possible to follow the kinetics of perpendicular charge movements.

The buffer in the compartments was made anaerobic by exchanging the gas atmosphere for N_2 and by using the glucose/glucose-oxidase/catalase system (25 mM, 1 U/ml, 20 U/ml) [34]. The N_2 atmosphere was then exchanged for 10–15% CO (see below), and NOR was reduced by the addition of ascorbate (2 mM) with 1 μM hexa-amineruthenium(II)-chloride (HARC) as the mediator. A jet of 40 μl NO- or O_2-saturated buffer was injected directly to the Teflon membrane, and the reaction initiated by a laser flash breaking the heme b_3-CO bond 0.5–1 s after starting the injection. The volume of the measuring cell allowed five injections per chamber. Usually the first two injections were with O_2-saturated (1.2 mM) buffer and the last three with NO-saturated (2 mM) buffer. To re-reduce NOR and consume O_2 or NO (by NOR and the asc/Gluc./GlOx/Cat. system) the solution was stirred for 10 min between each measurement.

The topology of the metal centers in NOR (see inset in Fig. 2) implies that for internal electron transfer in NOR, only those that move from heme *c* to heme *b* will create a potential, since all other electron movements are parallel to the membrane. The movement of negative charges from the outside of the vesicles into the bilayer will create a negative potential in our setup, whereas positive charges which move in the same direction give rise to a positive potential. The amplitude of the signal is proportional to the perpendicular distance that the charges move inside the membrane, the amount of charges that move inside each enzyme and the total amount of reacting enzymes.

2.5. Optical flow-flash studies

Liposome-reconstituted NOR was diluted to ~3 μM in a modified Thunberg cuvette, air was exchanged for nitrogen on a vacuum line, and the enzyme was reduced by adding ascorbate and HARC as above. This procedure results in reduction of only the 'right-side out' oriented NORs. Nitrogen was then exchanged for CO, after which the [CO] was lowered to 5–10% (in N_2) before the flow-flash studies in order to avoid CO recombination interfering with O_2 binding (see [19]).

Flow-flash measurements were performed on a set-up described in [35]. Briefly, the sample of fully reduced CO-bound v-NOR was mixed 1:1 with an oxygen-saturated ($[O_2]$ = 1.2 mM) buffer in a modified stopped-flow apparatus (Applied Photophysics). After a 200–400 ms delay a 10 ns laser flash (Nd-YAG laser, Quantel) was applied, dissociating CO and allowing O_2 to bind and initiate the reaction. The time course of the reaction was studied from μs-s at different wavelengths in the Soret and alpha regions. Typically, at each wavelength, 5×10^4 data points were collected and the data set was then reduced to ~1000 points by averaging over a progressively increasing number of points (logarithmic time scale).

For the proton uptake measurements, the v-NOR sample was passed through a PD-10 column (Pharmacia) equilibrated in 100 mM KCl, 0.5 mM EDTA, pH ~7.8. Phenol red at 40 μM was then added to the sample which was reduced and CO-equilibrated as above. If necessary, the pH was readjusted to ~7.8 as judged by the optical absorbance of the dye. In the flow-flash experiment, the O_2-saturated solution contained 100 mM KCl, 0.5 mM EDTA, and 40 μM phenol red at pH ~7.8. Absorbance changes of phenol red were monitored at 568 nm to minimise interference from absorbance changes due to oxidation of the hemes in NOR, as described in [19].

Because of the loss of total amount of NOR in the reconstitution procedure (of up to 50% of the starting amount), the sample size was not large enough to allow for titration of the buffering capacity of the exhaust from the flow-flash apparatus. Instead, since the same procedure is used here as that used in experiments with cytochrome *c* oxidase (C*c*O) [27], and since the lipids contribute much more to the total buffering capacity than the enzyme, we assume that the buffering capacity is approximately the same as in [27], with the correction that at 568 nm the signal change of phenol red is 60–70% of the maximum change occurring at 560 nm. The concentration of reacting NOR in the flow-flash experiment was obtained from the amplitude of the CO dissociation (at $t=0$) at 420 nm as described in [19].

For the pH-dependence measurements, the same 'de-buffered' v-NOR sample as for the proton uptake measurements was used and the oxygenated solution contained 100 mM Bis-Tris Propane (BTP) and 0.5 mM EDTA at the desired pH.

2.6. Data handling and analysis

To extract the rate constants of the observed phases in the flow-flash reaction, the time-resolved changes in absorbance were fitted either separately or globally (for data at different wavelengths) to a model of consecutive irreversible reactions (e.g. A→B→C) using the software package Pro-K (Applied Photophysics, UK). Alternatively, rate constants were fitted as a sum of exponentials in Sigmaplot (Jandel Scientific).

2.7. Construction of a 3D model of the NorB subunit from P. denitrificans

Modeling of the NorB subunit was performed essentially as done for the Pho84 phosphate transport protein described by Lagerstedt et al. [36] using the MetaServer platform (bioinfo.pl/meta/). The three highest ranked crystal structures judged by the 3D-Jury (Jscores: 202–199) [37]: 1m56 ([7] *R. sphaeroides* aa_3 oxidase), 1ar1 ([6]; *P. denitrificans* aa_3 oxidase) and 1fft ([8]; *E. coli* bo_3 oxidase), with sequence identities to the *P. denitrificans* NorB of ~15–20%, were used as templates to calculate structural models of NorB using the comparative modeling program MODELLER [38]. Each model was manually evaluated with the Visual Molecular Dynamics (VMD) software (Molecular Graphics Viewer) [39] by means of its three-dimensional helical arrangement and spatial positioning of the 6 conserved (presumed) metal-coordinating histidine ligands. The structural model based on the *E. coli* bo_3 oxidase structure was arbitrarily chosen for further treatment since all three models were very similar. Manual modifications using the parent coordinates and the program HyperChem 7.01 (for Windows, Hypercube) were made to provide the model with coordinates for the two *b*-type hemes and the non-heme Fe.

The model was then energy minimized using the Amber 8.0 program implementing a modified generalized Born solvation model [40] with a cut-off value of 16 Å using first restrained (harmonic force constant of 50 kcal/(mol*Å) for backbone and cofactor atoms) and then non-restrained conditions. The Amber force-field parameters (http://pharmacy.man.ac.uk/amber) were used for the heme groups. For Fe_B, a formal charge of +2, and sigma and van der Waals parameters the same as for the heme iron were used. The coordinates for the resulting working model are provided upon request.

Predictions of possible buried water molecules in the structural model were done using the DOWSER program [41]. The software searches for cavities with a suitable surrounding for a polar water molecule by measuring the interaction energies between the water molecule and the surrounding protein, and places water molecules in cavities with interaction energies below −12 kcal/mol. The process resulted in 32 predicted water molecules (strictly internal and surface-near) in the NorB model.

2.8. Sequence analysis

Sequences for NorB (~450 amino acids (aas)) and NorZ (~760 aas) from various organisms were retrieved from the NCBI protein database (http://www.ncbi.nlm.nih.gov). A set of sequences (see Supporting Material) for each class was imported into the Biology Workbench interface [42] and multiple sequence alignments (MSA) were calculated using the integrated CLUSTAL W program [43]. The two classes align over the whole NorB sequence, with the N-terminal extension in NorZ having no counterpart in the NorBs. The MSAs (found in the Supporting Material) were then used to search for residues conserved within both classes. Special focus was put on protonatable amino acids (Glu, Asp, Lys, Arg, His, Tyr, Thr and Ser) either fully conserved or where the properties of the residue in terms of charge/polarity remained at a ±1 position in the sequence.

3. Results

3.1. Proton uptake by liposome-reconstituted NOR during a few turnovers with O_2

NOR-liposomes ([NOR] ≅0.2 μM;) were mixed with a solution containing reduced cyt. *c* (10 μM) in the presence of oxygen and the pH-sensitive dye phenol red (Fig. 1). The

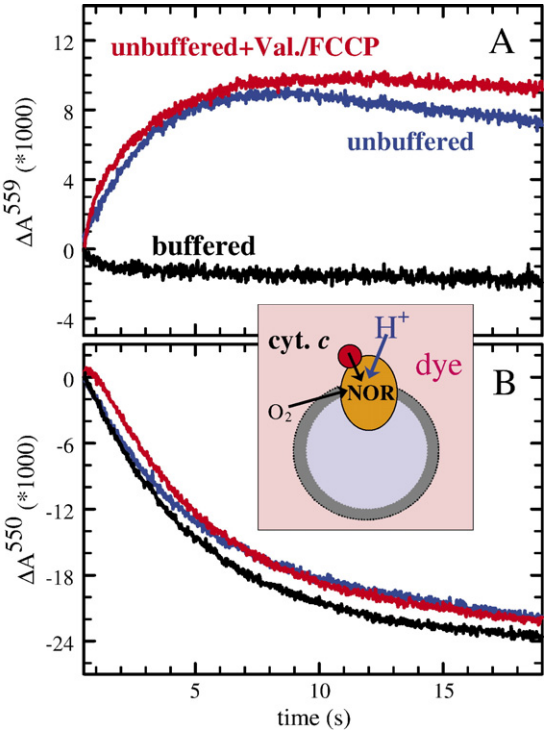

Fig. 1. Stopped-Flow measurements of pH changes outside v-NOR coupled to cyt. *c* oxidation during multiple (but less than 10) turnovers using O_2 as the substrate. (A) Uptake of protons, as shown by the absorbance increase at 559 nm of phenol red, added to the outside of the v-NOR. The wavelength 559 nm was chosen because it is the isobestic point of cyt. *c* oxidation, making the observed signals due only to changes in dye absorbance. The red and blue traces show the signals obtained in the absence of buffer, with (red trace) and without (blue trace) the uncouplers valinomycin and FCCP. The black trace shows the lack of signal obtained after addition of 10 mM HEPES buffer, pH 7.6. (B) Oxidation of cyt. *c*, measured at 550 nm. Note that the processes are coupled, i.e. occur with the same kinetics. The inset shows a schematic view of the experiment. Experimental conditions after mixing : ~0.1 μM v-NOR, 45 mM KCl, 45 mM sucrose, 0.5 mM EDTA, 50 μM phenol red, 5 μM reduced cyt. *c*, pH ~7.6, $T=298$K. (For interpretation of the references to colour in this figure legend, the reader is referred to the web version of this article.)

absorbance at 559 nm (of phenol red) increased due to an increase in pH, and concomitantly the absorbance at 550 nm decreased due to oxidation of cyt. *c*. No significant changes of the signals were observed in the presence of the uncouplers FCCP and valinomycin, indicating that no electrochemical gradient builds up during the experiment. Using the determined buffering capacity of the exhaust from the stopped-flow apparatus, and a $\Delta\varepsilon^{550}$(red-ox)=21 mM^{-1} for cyt. *c*, we obtain a proton/electron ratio of roughly 1–2, where 1 is the expected value (see Eq. (2a)) if the protons used for oxygen reduction originate from the 'outside' solution.

3.2. Electrometric potential generation during single turnover reduction of NO and O_2 by fully reduced NOR

Movement of charge perpendicular to the membrane in v-NOR was studied during oxidation of the fully reduced enzyme, using the flow-flash technique in combination with an electrometric detection technique. Buffer saturated with either NO or O_2 was injected into the chamber containing fully reduced CO-bound v-NOR attached to the measuring membrane, and CO was flashed off allowing the substrate (NO or O_2) to bind and initiate the reaction. Since fully reduced NOR contains four electrons, this experiment should give one turnover with O_2 (requiring four electrons to be reduced to H_2O) and two turnovers with NO (requiring two electrons to be reduced to N_2O).

For NO as a substrate, our results (shown in Fig. 2) are very similar to those obtained by Hendriks et al. [25], i.e. a rapid development of negative potential followed by a larger positive voltage change with a time constant of 3–5 ms (at pH 7.5), or alternatively with two components with time constants of 1.7 and 10 ms (c.f. [25]). Because of the way the electrodes are 'set up', and the arrangement of the cofactors in NOR (see inset in Fig. 2 and [25]), movement of electrons from the low-spin heme

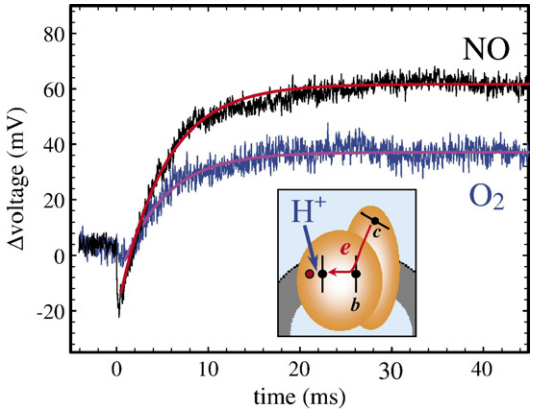

Fig. 2. Generation of electrical potential during the reaction between fully reduced v-NOR and either NO (black trace) or O_2 (blue trace). After injection of either NO- or O_2-saturated buffer into the chamber, a laser flash breaks the CO-bond at $t=0$ to initiate the reaction. The red and purple curves are fits (starting at 0.5 ms) to the traces with the same rate constant $k=200\ s^{-1}$ ($\tau=5$ ms). Buffer used: 100 mM HEPES, pH 7.5. For experimental details, see Materials and methods. The inset shows the topology of the redox sites and illustrates that the net positive signal is presumably due to more protons than electrons being transferred. (For interpretation of the references to colour in this figure legend, the reader is referred to the web version of this article.)

c to heme *b* should generate a negative potential, movement from the low-spin heme *b* into the active site should be electrically silent, and movement of protons into the active site should give a negative signal if they originate from the inside, and a positive signal if from the outside. The net positive potential generation observed in our experiments is thus presumably due to a larger extent of proton movements in the same direction as electron movement, i.e. from the outside.

Using O_2 as a substrate, the results are qualitatively very similar to the results with NO, i.e. net generation of positive potential, with a $\tau=5$–10 ms at pH 7.5 (Fig. 2). The only obvious difference from the NO signals is the disappearance of the rapid negative signal (see Fig. 2). With O_2, there is only a lag phase that precedes the build-up of positive potential, see Discussion.

The amplitudes of voltage generation vary between experiments and are not easily calibrated in terms of number of charges moving. However, for NOR the amplitudes were 5–10% of those obtained with C*c*O (in the opposite, negative direction) using the same procedure (Lepp et al. manuscript). In C*c*O, the net movement of charge during oxidation of the reduced enzyme is presumably −3.5 charges (see e.g. [44]), suggesting that the amplitudes in NOR correspond to +0.2–0.4 charges. In the optical flow-flash reaction between reduced s-NOR and O_2, we estimated that ~50% of the electron on heme *c* moved to the active site during the 25-ms phase (corresponding presumably to the electrogenic $\tau=5$–10 ms phase), and that ~1H^+/NOR was taken up from solution [19]. Assuming the same stoichiometry in the electrometric reaction of v-NOR, and that the proton comes from the periplasm, this would give rise to a net movement of half a positive charge halfway through the membrane dielectric (assuming for simplicity that the active site in NOR is situated at a depth halfway through the membrane-spanning region), resulting in a net charge movement of +0.25, which fits well with the observed amplitudes.

The rate constant for relaxation of the built-up potential back to the zero level in the electrometric set-up depends partly on the tightness of the fused membrane vesicles, such that it puts an upper limit on the rate constant for proton leakage. This relaxation rate constant was 2–5 s^{-1} (data not shown), indicating well-sealed vesicles, such that this process did not interfere with the observed signals on the ms time-scale. However, this relaxation rate made it impossible to resolve any charge movements during the ~1 s^{-1} phase of electron transfer observed in the optical measurements ([19], and see below).

3.3. Single turnover proton uptake during O_2-reduction by fully reduced liposome-reconstituted NOR

In the electrometric studies, only charge movements across the membrane dielectric, i.e. internally, are observed. For proton transfer into the active site, it is thus not possible to distinguish a proton that originates from inside the protein from a proton that is transferred from the bulk solution. Therefore, we also investigated the reaction between fully reduced v-NOR and O_2 optically, and used a pH-sensitive dye (phenol red) added to the outside of the vesicles in order to directly study H^+ uptake from solution.

First, we compared the reaction in v-NOR to that in s-NOR [19] at 430 nm where both the O_2-binding (τ=40 μs in s-NOR) phase and the subsequent heme oxidation phase (τ=25 ms at pH 7.5 in s-NOR) are clearly seen, see Fig. 3. The results show that, within the experimental error, the 2nd order rate constant for O_2 binding was the same in v-NOR as in s-NOR. The proton-coupled electron transfer (τ=25 ms in s-NOR) was accelerated slightly to ~15 ms (at pH 7.5) in v-NOR, and the amplitude was slightly larger. The slower phase of heme oxidation with τ ~1 s observed previously in s-NOR [19] is seen also in v-NOR (data not shown).

Direct measurements of proton uptake from outside reported by changes in absorbance of phenol red at 568 nm showed an increase in the dye absorbance with a τ=17 ms (at pH ~7.8), the same time constant was observed for heme oxidation at 420 nm in the same experiment (see Fig. 4). This result shows that proton uptake coupled to the τ ~15 ms electron transfer occurs from the outside of the vesicles (cf. the periplasmic solution). Using the approximation described in Materials and methods, the amplitude of the dye signal corresponds to ~1–$2H^+$/reacting NOR. Since in s-NOR, ~$1H^+$/reacting NOR is taken up from the bulk solution [19], all protons in the reaction come from the outside.

The slow pH decrease with k ~3 s^{-1} (see fit in Fig. 4) is presumably due to a leakage of protons from the inside to the outside of the vesicles, since a maximum rate constant for proton leakage of 2–5 s^{-1} was obtained in the electrometric measurements (see above).

We also studied the 15-ms phase in v-NOR at several pHs by mixing, in the flow-flash setup, a buffer-free v-NOR solution with different buffers of desired pH. The results (see inset in Fig. 4) show that the pH dependence measured in this way for v-NOR is very similar to the dependence in s-NOR [19], with a slight shift to either a higher maximum rate constant or a higher pK_a. Since the experimental procedure leaves only 200–400 ms between mixing and initiating the measurements, we assume that the pH inside the vesicles has not had time to change significantly, which means that NOR responds to pH on the outside of the vesicles similarly to the way s-NOR responds to changes in bulk pH. This result is a further indication that protons are taken up from outside.

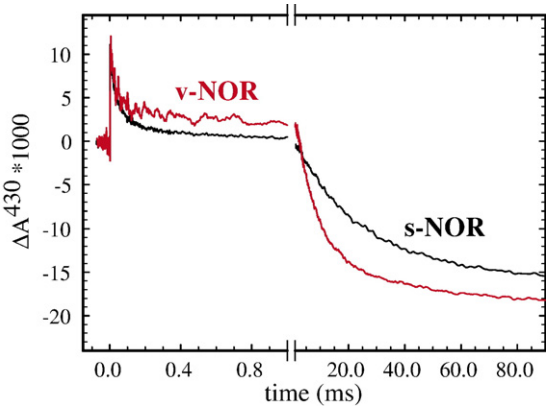

Fig. 3. The reaction between fully reduced NOR and O_2 showing the comparison between the reaction in solubilised (s-NOR, black trace, data from [19]) and liposome-reconstituted NOR (v-NOR, red trace). A laser flash initiates the reaction at t=0. Shown are the absorbance changes at 430 nm, where both the O_2 binding phase (τ=40 μs at 1 mM O_2 in s-NOR) and the heme oxidation phase (τ =25 ms in s-NOR) are clearly seen. These phases were fitted to τ=60–80 μs (at 0.6 mM O_2) and τ =15 ms in v-NOR. Experimental conditions: ~1 μM reacting NOR in 100 mM HEPES–KOH, pH 7.5, (+50 mM KCl, 0.05% DDM for s-NOR) [O_2]=1 mM (s-NOR) or 0.6 mM (v-NOR), T=298 K. The laser flash at t=0 gives an artifact that has been truncated for clarity. (For interpretation of the references to colour in this figure legend, the reader is referred to the web version of this article.)

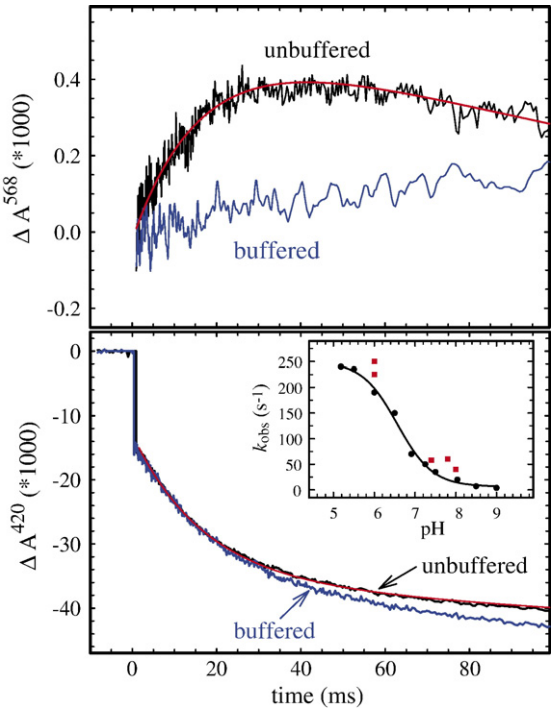

Fig. 4. Proton uptake coupled to heme oxidation during the reaction between fully reduced v-NOR and O_2. (Top panel) Absorbance changes at 568 nm of phenol red (black trace), added to the outside of the liposomes, corresponding to proton uptake from outside. The red trace is a two-exponential fit to the data with k_1= 60 s^{-1} (τ= 17 ms) and a slower drift (or proton leakage) with k_2= 3–4 s^{-1} (τ=0.2–0.3 s). The changes in absorbance are shown between 0.5 and 90 ms to emphasize the τ=17 ms phase. The wavelength 568 nm was chosen in order to minimize the contribution from redox reactions in NOR (see [19]), as confirmed by the disappearance of the τ=17 ms phase in the presence of buffer (blue trace). (Lower panel) Absorbance changes (in the same experiment) at 420 nm, where oxidation of the heme groups is seen. The red trace is a fit to the unbuffered trace with the same rate constants as in the top panel, where the k= 3–4 s^{-1} phase is further heme oxidation. Experimental conditions: ~0.5 μM reacting NOR in 100 mM KCl, 0.5 mM EDTA, 40 μM phenol red, pH ~7.8, [O_2]=0.6 mM, T=298 K. The inset in the lower panel shows the pH-dependence of the 25 ms phase in s-NOR (black circles, data from [19]) and data obtained for v-NOR (red squares). For experimental details, see text. The black line is the fit to the dependence in s-NOR to a pK_a = 6.6 and a k_{max}=250 s^{-1} [19]. (For interpretation of the references to colour in this figure legend, the reader is referred to the web version of this article.)

3.4. 3D NorB model

An overview of the generated model for the *P. denitrificans* NorB, based on the structure of the bo_3 oxidase from *E. coli* [8] is shown in Fig. 5A. The general topology of the NOR transmembrane helices has been demonstrated in *Pseudomonas*

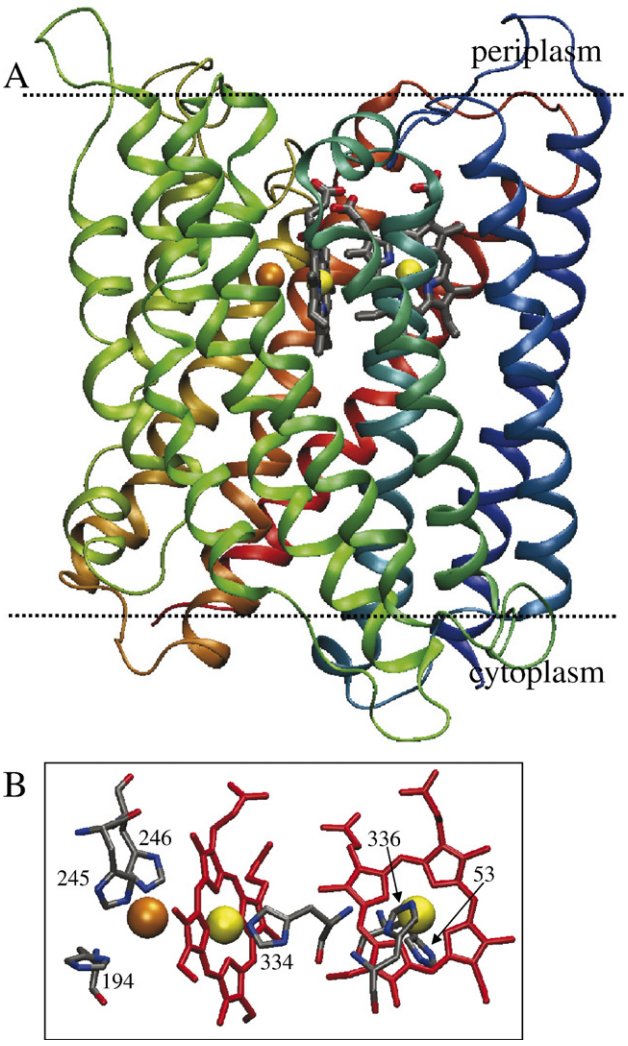

Fig. 5. Structural model of NorB from *P. denitrificans*. (A) Overview of the 12-helical structure and cofactors. The 12 helices are colour-coded from the N-(red) to the C- (blue) terminal. The low-spin heme *b* is to the right, and the high-spin heme b_3 and the non-heme Fe_B (orange) to the left. The approximate location of the membrane is indicated. (B) Close-up of the area around the cofactors showing the conserved (among all HCuOs) histidine ligands. The view is the same as in A. The pictures were made using the VMD software [39]. (For interpretation of the references to colour in this figure legend, the reader is referred to the web version of this article.)

stutzeri [45]. Fig. 5B shows the coordination of the conserved histidine ligands to the cofactors (heme *b*, heme b_3 and Fe_B). One of the uncertainties in modeling the NorB active site on subunit I of HCuOs is the coordination sphere of Fe_B, since in contrast to the three-histidine ligated Cu_B, non-heme irons are known to prefer octahedral ligation with one or more O-ligands [2]. In the generated model, no carboxyl (Glu or Asp) or hydroxyl (Ser or Thr) side-chains are close enough to Fe_B to provide an additional ligand. The closest amino acids as candidates for additional ligands are Glu-267 and Glu-198 with the carboxylic acid oxygens on average 7 Å and 9 Å, respectively, from Fe_B, and the hydroxyls of Thr-243 and Ser-264 both about 6.5 Å from Fe_B (see Fig. 6). This lack of putative additional ligands was observed also in the model of the *P. stutzeri* NorB [1,45]. Overall, our modeled structure is very similar to the model of the *stutzeri* NorB, as determined by the backbone helical arrangement (rmsd: 1.26 Å). The presumed O-ligand requirement of Fe_B could be fulfilled also

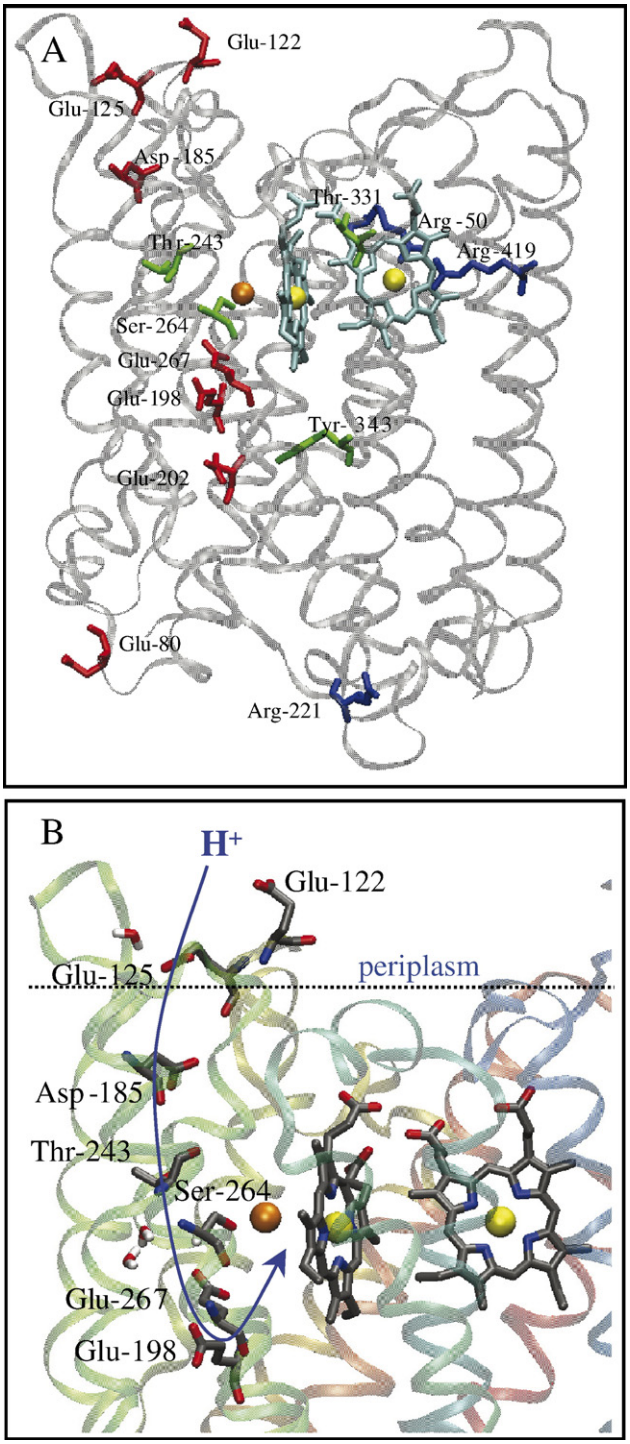

Fig. 6. (A) Same view as in Fig. 5 but showing the location of conserved (among both NorB and NorZ) protonatable amino acids. The acidic residues are in red, basic in blue and hydroxyls in green. (B) Close-up of the region between the outer surface of the protein and the catalytic heme b_3-Fe_B site where a route for protons should be located. The suggested pathway, including predicted water molecules in the area, is indicated. (For interpretation of the references to colour in this figure legend, the reader is referred to the web version of this article.)

by water or hydroxide ligands, and there is space for a water molecule ~6 Å from Fe_B, as placed by DOWSER. It should be noted, however, that modeled water molecules in a modeled structure are inevitably very uncertain.

When looking for possible pathways for protons into the heme b_3-Fe_B active site in the NorB model, we first searched a set of NorB/NorZ sequences for conserved or functionally similar protonatable amino acids (the alignments are found in the Supporting Material) in the whole subunit. Out of the thus identified residues (see Fig. 6A) residues Arg-50, Glu-122, Glu-198, Glu-202, Ser-264, Glu-267, Tyr-343, Arg-419 are completely conserved, Thr-331 is changed to Ser in one sequence, Glu-80 and Glu-125 are changed to Asp in some sequences, Asp-185 is changed to Glu or 'moved' to position 186 in some sequences, Arg-221 is changed to a Lys or 'moved' to position 222 in some sequences, and Thr-243 is conserved in all except one sequence.

Of these conserved protonatable residues, Arg-50 and Arg-419 presumably stabilize the propionates of the low-spin heme *b* (see Discussion). The Arg-221 and the Glu-80 are both located at the cytoplasmic surface. Except for the Tyr-343 and Glu-202, the other conserved protonatable residues are located above (i.e. towards or at the periplasmic surface of the protein), or close to, the heme b_3-Fe_B active site. We then focused in on this region, since our data show that protons are taken up from this side of the membrane (see above).

Fig. 6B shows our suggested operating pathway for protons, which consists of all remaining protonatable residues and possibly a few modeled water molecules. At the periplasmic surface in our model of NorB, the only conserved protonatable residues that could be acting as the entry points for protons are the Glu-122 and Glu-125, located ~30 Å from the heme b_3-Fe_B active site. The distance from these surface residues to the next conserved protonatable residue, Asp-185 is quite long, ~15 Å (see Discussion). Next is the Thr-243 ~13 Å from the Asp-185. The Thr-243 is at 6.5 Å from Fe_B, as noted above when considered as a potential ligand to it. In the area is also Ser-264, 7.5 Å from the Thr-243 and 6.4 Å from Fe_B, and a cluster of three modeled water molecules at 6–9 Å from Fe_B and at the closest 3 Å from Ser-264. The other conserved residues in the area are Glu-267 and Glu-198 with their shortest distances to other groups being 4 Å (Glu-267 to Ser-264) and 4.8 Å (Glu-267 to Glu-198). The Glu-198 is ~9 Å from Fe_B.

4. Discussion

In this study we have shown, by direct measurements in the liposome-reconstituted protein, that bacterial nitric oxide reductase takes its substrate protons from the periplasmic side of the bacterial membrane. The results were obtained using oxygen as the substrate instead of NO as O_2 is much more amenable to the unbuffered solutions needed for direct measurements of pH changes. The validity of using O_2 as a model substrate for proton transfer measurements was shown using an electrometric technique. Further, we constructed a 3D-model of the catalytic subunit NorB in order to search for plausible pathways for protons leading from the periplasmic surface into the active site. Such pathways should consist of conserved protonatable residues and/or water molecules. The experimental data and the suggested pathway is discussed further below.

4.1. Proton uptake in vesicle-reconstituted NOR

During NOR turnover with reduced cyt. *c* as the electron donor and O_2 as the oxidant, there is a pH increase outside of the vesicles concomitant with cyt. *c* oxidation (see Fig. 1). These results are consistent with NOR using protons from the outer (periplasmic) solution, as are the RCRs (see Materials and methods) which were =1 for both NO (as observed previously [25]) and O_2.

In order to study individual reaction steps in the catalytic cycle that specifically involve proton transfer we monitored the single turnover oxidation of the fully reduced enzyme using the flow-flash technique in combination with both an electrometric detection technique and optical spectroscopy. The electrometric technique is sensitive to internal charge transfers perpendicular to the membrane, but not transfer from the bulk solution to the surface of the protein. Therefore, the solutions used may be buffered, and NO can be used as a substrate. This gave us the possibility to compare results with NO and O_2 in order to validate the use of O_2 as a model substrate when studying proton transfer in NOR. Our results with NO as the substrate (Fig. 2) are in good agreement with those obtained by Hendriks et al. [25], i.e. a net build-up of positive potential, in our case fitted to a time constants of ~5 ms (pH 7.5). Since transfer of electrons internally from heme *c* to heme *b* should give rise to negative potential, and transfer from heme *b* into the active site is presumably non-electrogenic, the positive potential most likely originates from proton transfer from the outer surface, either internally, or taken up from solution. There must be more protons transferred than electrons moving from heme *c*, since a net positive signal is observed. Before the build-up of positive potential, there is a small rapid signal of opposite sign, observed also by Hendriks et al. [25] that, as they observed no link to electron transfer from heme *c* until the later phases, they interpreted as movement of a charged amino acid concomitant with oxidation of the active site during the first two-electron turnover of NO to N_2O.

When O_2 is the substrate, positive potential builds up with a τ of 5–10 ms (pH 7.5), i.e. similar to when NO is the substrate. This time constant is close to that observed optically for the proton-coupled electron transfer reaction in v-NOR (τ=15 ms, see below). In s-NOR, we estimated that the corresponding τ=25 ms phase involved oxidation of ~50% of heme *c* and uptake of ~$1H^+$/NOR [19]. Because a net positive signal is observed, the proton must come from the outer surface. Thus, internal proton-transfer reactions in NOR are approximately the same regardless of whether NO or O_2 is used as the substrate, showing that O_2 is a good model substrate for investigating proton-transfer reactions in NOR. Furthermore, since the time constants are so similar, it is likely that the actual transfer of protons is rate-limiting for the reactions on the ms time scale with both NO and O_2 (as suggested earlier [19]).

There is no rapid signal with negative sign in the reaction with O_2, which is in good agreement with our optical data for s-NOR, which showed no evidence for any reaction occurring between the binding of O_2 (τ=40 μs at 1 mM O_2) and the proton-coupled electron transfer (τ=25 ms) [19]. Instead a lag phase precedes the τ=5–10 ms electrogenic phase, which we suggest corresponds to the electrically silent binding of O_2.

It should be noted that the flow-flash reaction involves only the oxidative part of the NOR turnover. Because a net positive potential is generated in this part, a net negative potential is presumably generated in the reductive phase, resulting in a turnover reaction that is overall electrically silent, as observed by Hendriks et al. [25]. This in turn means that during reduction of NOR, not all electrons moving into heme *b* (and onto the active site) are charge-compensated by proton uptake. This scenario might have a physiological role in that the oxidative part of the reaction that involves binding and reduction of the toxic NO molecule works 'downhill' the existing proton gradient whereas the reductive part works 'uphill'.

Since the electrometric technique measures internal charge transfer and not net uptake of protons from solution, we also studied the flow-flash reaction between fully reduced liposome-reconstituted NOR and O_2 using optical detection of changes in external pH, reported by phenol red. The results show an absorbance increase of the dye (Fig. 4) concomitant with the oxidation of the heme groups (τ=15 ms at pH 7.5, see Figs. 3 and 4), as observed with the s-NOR. As the dye is only added to the outside of the vesicles and the reaction is rapid enough to not allow protons to back-leak into the vesicles (as shown by the relaxation rates in the electrometric measurements, see Results), these results show that protons needed for the reduction of O_2 (see Eq. (2a)) are indeed taken up from the solution on the outside of the vesicles. Taken together with the similarity between NO and O_2 in the electrometric data, these results strongly indicate that protons for NO-reduction are also supplied from the outside.

Furthermore, when the pH is rapidly changed outside the v-NOR, the observed pH-dependence of the rate constant associated with proton uptake (see inset in Fig. 4) is very similar to the pH-profile obtained in s-NOR [19], supporting that the protons are taken from outside, since the pH inside the vesicles is not expected to change substantially during the mixing time.

4.2. Proton transfer into the heme b_3-Fe_B site; mechanism and pathway

Having confirmed that protons are taken up from the outer (periplasmic) solution into the active site, we can speculate about the location of the proton-transfer pathway and about the identity of the internal proton donor (with pK_a=6.6) to the active site.

Fig. 6A shows all protonatable groups that are conserved or functionally similar in the NorB/NorZ alignments (see Materials and methods). Of these conserved protonatable residues, Arg-50 and Arg-419 presumably stabilize the propionates of the low-spin heme *b*, as the distance in the model is about 6 Å for both Arg-propionate pairs. In the NorB sequences, there is an additional Arg (399), which aligns with Arg-482 of the A1 type HCuOs in which it stabilises the low-spin heme.

Arg-221 and Glu-80 are both located at the cytoplasmic surface, and interestingly, Glu-80 actually aligns (see alignments in [46]) with the Asp-132 of the A1 HCuOs, in which it is the crucial initial proton donor for (and gives the name to) the D-pathway that conveys both substrate and pumped protons. The Asp-132 is not conserved among all HCuOs, it is e.g. absent in the *cbb*$_3$-type oxidases, which are closer relatives to NOR, raising questions about the evolution of the super-family, and about plausible roles of the Glu-80 in the NORs.

Except for the Tyr-343 and Glu-202, the other conserved protonatable residues are located above (i.e. towards or at the periplasmic surface of the protein), or close to, the heme b_3-Fe_B active site. We then focused on this region, since our data show that protons are taken up from this side of the membrane (Fig. 4).

Fig. 6B shows our suggested operating pathway for protons, which consists of all remaining protonatable residues (see above) and a few putative, modeled water molecules. The suggested entry point for protons is at the Glu-122/Glu-125 pair, located ~30 Å from the heme b_3-Fe_B active site. These glutamates are the only conserved protonatable residues at the periplasmic surface in our NorB model. The importance of the Glu-122 and Glu-125 for catalytic activity has been tested by site-directed mutagenesis [18,47] and were found to be essential for normal steady-state NO-reduction activity without affecting the expression of the protein. As these residues are located far from the active site, a role for them in proton transfer is likely. The other conserved glutamic acid residues whose importance also have been tested using site-directed mutagenesis, Glu-198, Glu-202 and Glu-267 [18,47] are located at the 'other end' of (Glu-198, Glu-267) or are not part of (Glu-202) the suggested pathway. The Glu-198 and Glu-267 are located slightly below the active site, at 9 and 7 Å from Fe_B, respectively, and were both found to be essential for steady-state activity without affecting the assembly of the NOR [18,47]. It cannot be excluded that at least one of these Glus acts as a Fe_B ligand, but since in our model, they are both too far away for this role, we suggest that they are likely to form part of the proton-transfer pathway. The Glu-202/Ala mutant NOR retains 30% catalytic activity [18], and is situated quite far below the active site (see Fig. 6, distance to Fe_B ~15 Å), which is why we have excluded it from the suggested pathway.

The E122/125 couple is ~30 Å from the Glu198/267, a distance that needs to be bridged by other protonatable residues and/or water molecules. The distance from the surface glutamates (122, 125) to the next ('down' towards the active site) conserved protonatable residue, Asp-185, is quite long, ~15 Å, which decreases to ~9 Å if a water molecule (see Fig. 6B) and the Arg-121 (not shown in the figure, since it is a Tyr in some sequences) is presumed to participate. Also the next protonatable residue, Thr-243 (6.5 Å from Fe_B) is quite some distance from Asp-185, ~13 Å. In the area is also a Ser-264, 7.5 Å from the Thr-243 and 6.4 Å from Fe_B, and a cluster of three modeled water molecules at 6–9 Å from Fe_B and the closest 3 Å from Ser-264. The distance from these residues to the essential glutamates (198, 267) is at the closest ~4 Å (Ser-

264 to Glu-267). We have included the Glu-198 and Glu-267 in the suggested pathway although other residues (like Ser-264) are closer to the active site because of the Glu-198 and Glu-267 them being essential for catalytic activity and because they provide a more likely candidate for the pK_a=6.6 internal proton donor identified previously [19].

It should be noted that quite a few distances between groups in this pathway are too long for hydrogen bonding, so that either more water molecules (or more protonatable groups), or conformational changes would be needed for efficient proton transfer. In this context it is relevant to note that in the D-pathway of the A1 HCuOs, the major part of the proton connectivity is provided by water molecules stabilised by polar amino acids, which can be individually mutated without changing the observed proton transfer rates [7,48,49,50]. Furthermore, in the D-pathway, the connection from Glu-286 onwards is unclear, and unresolved water molecules as well as conformational changes have been suggested to bridge the gap to the proton acceptor (see e.g. [6,51]).

It should also be noted that we included both long-chain NorZ and short-chain NorB sequences in our alignments, where the NorZ proteins presumably use quinol as the electron donor, instead of water-soluble electron donors such as cyt. *c*. As quinol is oxidised to quinone, it releases two protons, leading to the possibility that the NorZ and the NorB proteins have different proton pathways, with the one for NorZ leading from the quinol-oxidizing site into the active site. Taking this possibility into account, we searched also for plausible components of the proton transfer pathway conserved only among the short-chain NorB sequences (alignments not shown), and found a few residues that could increase the connectivity of the suggested pathway; Lys-186 (the residue after Asp-185 in the sequence and located ~7.5 Å from it) and Thr-317, located about 5.5 Å from Ser-264.

We can also speculate about the possible relationship between the 'input' path for protons in the NORs and the output path for pumped protons in HCuOs, which is largely unknown. Interestingly, in the *cbb*$_3$ oxidases, the HCuOs with the highest sequence similarity to the NORs, the Glu-122 and Glu-125 are conserved, whereas they are not in the A1 HCuOs (as seen from the alignments in [46]). It is thus possible that these glutamates are involved in the release of pumped protons in the *cbb*3 s, something that is currently being tested by site-directed mutagenesis (R. Gennis, personal communication).

When it comes to the pK_a=6.6 group shuttling protons into the heme b_3-Fe_B site (see above), Glu-198 is a good candidate. This is partly because it sits close (~9 Å) to Fe_B and also because, interestingly, the Glu-198 forms part of a conserved motif [2] around one of the predicted His ligands (H194) to Fe_B in the NORs; **H**LWV**E**G. The A1 HCuOs also have a conserved motif around one of the His ligands (H284) to Cu_B; G**HPE**VY. Here, the glutamate is Glu-286, a residue shown to be crucial for, and limiting the rate of, proton transfer into the active site [22,52–56]. It is thus tempting to suggest that Glu-198 has the corresponding function in the NORs.

We are currently investigating if proton uptake is indeed specifically inhibited in the mutant NORs with the Glus exchanged (Glu-198, Glu-202, Glu-122, Glu-125), and the role of other components of the suggested pathway can be tested by further site-directed mutagenesis, the guiding for which our model serves as a platform.

4.3. Why is NOR not a proton pump?

The free energy available from NO-reduction (E'_0=1.2 V) is comparable to that available to the O_2-reducing (E'_0=0.8 V) heme-copper oxidases. Despite this, the NORs are not proton pumps, and, as shown by direct measurements in this work, the substrate protons are consumed from the same side as the electrons, leading to a completely non-electrogenic reaction. There are several possible reasons for this behavior. First, NO is a very toxic molecule, the steady-state concentration of which is kept low (in the nM range [57]) in the denitrifying bacterium. This could mean that the mechanism of NO-reduction (to N_2O, which is much less toxic) has evolved into rapidly removing NO rather than conserving energy, since an efficient pump would work close to equilibrium, i.e. consume NO relatively slowly. The low steady-state concentration of NO also results in a lower free energy available from its reduction, but even at [NO]=1 nM, the actual *E* is at least as high as that for reducing O_2.

There could also be a more basic chemical reason for not coupling NO-reduction to proton pumping, which is related to the pK_as of the intermediates formed at the catalytic site. In a theoretical study of NO-reduction, the proton affinities of the suggested intermediates were low [58], which means that the driving force for proton transfer into the active site is low, and therefore difficult to use to drive the energetically uphill transfer of protons against the chemical gradient. In contrast, in HCuOs, the pK_as of the intermediates during O_2-reduction are very high (see e.g. [59]), which makes protonation of these intermediates favorable, something that can be used as a driving force for the pumping mechanism.

Since the NORs do not conserve energy, one might ask why they are membrane-bound proteins? This question is related to the course of evolution of the heme-copper oxidases. This course is not clear in terms of the common ancestor, what was its catalytic specificity? And did it pump protons? It has been suggested that the ancestor was reducing NO [3], partly because NO was probably much more abundant in the early atmosphere than O_2 was before photosynthesis. Although very attractive, this scenario has been questioned on the basis of alignments of the increasing number of available HCuO sequences [15]. If the NORs evolved from a primordial oxygen-reducing HCuO, then it being a membrane protein might simply be an 'evolutionary artifact' of it being a HCuO.

Acknowledgements

Mattias Blomberg and Margareta Blomberg (Stockholm University) are acknowledged for help with energy minimizations of the NorB model. We thank Nick Watmough (University of East Anglia) for helpful discussions as well as for the NOR plasmids and strains, Kristina Faxén (Stockholm

University) for advice on liposome reconstitution, and Walter Zumft (University of Karlsruhe) for sending us the publication on, as well as the coordinates for the *P. stutzeri* NorB model. These studies were financially supported by The Swedish Research Council.

Appendix A. Supplementary data

Supplementary data associated with this article can be found, in the online version, at doi:10.1016/j.bbabio.2007.03.006.

References

[1] W.G. Zumft, Nitric oxide reductases of prokaryotes with emphasis on the respiratory, heme-copper oxidase type, J. Inorg. Biochem. 99 (2005) 194–215.
[2] N.J. Watmough, G. Butland, M.R. Cheesman, J.W. Moir, D.J. Richardson, S. Spiro, Nitric oxide in bacteria: synthesis and consumption, Biochim. Biophys. Acta 1411 (1999) 456–474.
[3] M. Saraste, J. Castresana, Cytochrome oxidase evolved by tinkering with denitrification enzymes, FEBS Lett. 341 (1994) 1–4.
[4] J. van der Oost, A.P. de Boer, J.W. de Gier, W.G. Zumft, A.H. Stouthamer, R.J. van Spanning, The heme-copper oxidase family consists of three distinct types of terminal oxidases and is related to nitric oxide reductase, FEMS Microbiol. Lett. 121 (1994) 1–9.
[5] T. Tsukihara, H. Aoyama, E. Yamashita, T. Tomizaki, H. Yamaguchi, K. Shinzawa-Itoh, R. Nakashima, R. Yaono, S. Yoshikawa, The whole structure of the 13-subunit oxidized cytochrome *c* oxidase at 2.8 Å, Science 272 (1996) 1136–1144.
[6] S. Iwata, C. Ostermeier, B. Ludwig, H. Michel, Structure at 2.8 Å resolution of cytochrome *c* oxidase from *Paracoccus denitrificans*, Nature 376 (1995) 660–669.
[7] M. Svensson-Ek, J. Abramson, G. Larsson, S. Törnroth, P. Brzezinski, S. Iwata, The X-ray crystal structures of wild-type and EQ(I-286) mutant cytochrome *c* oxidases from *Rhodobacter sphaeroides*, J. Mol. Biol. 321 (2002) 329–339.
[8] J. Abramson, S. Riistama, G. Larsson, A. Jasaitis, M. Svensson-Ek, L. Laakkonen, A. Puustinen, S. Iwata, M. Wikström, The structure of the ubiquinol oxidase from *Escherichia coli* and its ubiquinone binding site, Nat. Struct. Biol. 7 (2000) 910–917.
[9] T. Soulimane, G. Buse, G.P. Bourenkov, H.D. Bartunik, R. Huber, M.E. Than, Structure and mechanism of the aberrant ba(3)-cytochrome *c* oxidase from *Thermus thermophilus*, EMBO J. 19 (2000) 1766–1776.
[10] J. Hendriks, A. Warne, U. Gohlke, T. Haltia, C. Ludovici, M. Lübben, M. Saraste, The active site of the bacterial nitric oxide reductase is a dinuclear iron center, Biochemistry 37 (1998) 13102–13109.
[11] P. Girsch, S. deVries, Purification and initial kinetic and spectroscopic characterization of NO reductase from *Paracoccus denitrificans*, Biochim. Biophys. Acta 1318 (1997) 202–216.
[12] R. Cramm, A. Pohlmann, B. Friedrich, Purification and characterization of the single-component nitric oxide reductase from *Ralstonia eutropha* H16, FEBS Lett. 460 (1999) 6–10.
[13] P. Brzezinski, P. Ädelroth, Design principles of proton-pumping haem-copper oxidases, Curr. Opin. Struct. Biol. 16 (2006) 465–472.
[14] P. Brzezinski, Redox-driven membrane-bound proton pumps, Trends Biochem. Sci. 29 (2004) 380–387.
[15] M.M. Pereira, M. Santana, M. Teixeira, A novel scenario for the evolution of haem-copper oxygen reductases, Biochim. Biophys. Acta 1505 (2001) 185–208.
[16] S. Ferguson-Miller, G.T. Babcock, Heme-copper terminal oxidases, Chem. Rev. 96 (1996) 2889–2907.
[17] T. Fujiwara, Y. Fukumori, Cytochrome cb-type nitric oxide reductase with cytochrome *c* oxidase activity from *Paracoccus denitrificans* Atcc 35512, J. Bacteriol. 178 (1996) 1866–1871.
[18] G. Butland, S. Spiro, N.J. Watmough, D.J. Richardson, Two conserved glutamates in the bacterial nitric oxide reductase are essential for activity but not assembly of the enzyme, J. Bacteriol. 183 (2001) 189–199.
[19] U. Flock, N.J. Watmough, P. Ädelroth, Electron/proton coupling in bacterial nitric oxide reductase during reduction of oxygen, Biochemistry 44 (2005) 10711–10719.
[20] C.A. Wraight, Chance and design—proton transfer in water, channels and bioenergetic proteins, Biochim. Biophys. Acta 1757 (2006) 886–912.
[21] P. Brzezinski, P. Ädelroth, Pathways of proton transfer in cytochrome *c* oxidase, J. Bioenerg. Biomembr. 30 (1998) 99–107.
[22] A.A. Konstantinov, S. Siletsky, D. Mitchell, A. Kaulen, R.B. Gennis, The roles of the two proton input channels in cytochrome *c* oxidase from *Rhodobacter sphaeroides* probed by the effects of site-directed mutations on time-resolved electrogenic intraprotein proton transfer, Proc. Natl. Acad. Sci. U. S. A. 94 (1997) 9085–9090.
[23] J.P. Shapleigh, W.J. Payne, Nitric oxide-dependent proton translocation in various denitrifiers, J. Bacteriol. 163 (1985) 837–840.
[24] L.C. Bell, D.J. Richardson, S.J. Ferguson, Identification of nitric oxide reductase activity in *Rhodobacter capsulatus*: the electron transport pathway can either use or bypass both cytochrome *c*2 and the cytochrome bc1 complex, J. Gen. Microbiol. 138 (1992) 437–443.
[25] J.H. Hendriks, A. Jasaitis, M. Saraste, M.I. Verkhovsky, Proton and electron pathways in the bacterial nitric oxide reductase, Biochemistry 41 (2002) 2331–2340.
[26] U. Flock, J. Reimann, P. Ädelroth, Proton transfer in bacterial nitric oxide reductase, Biochem. Soc. Trans. 34 (2006) 188–190.
[27] K. Faxén, G. Gilderson, P. Ädelroth, P. Brzezinski, A mechanistic principle for proton pumping by cytochrome *c* oxidase, Nature 437 (2005) 286–289.
[28] A. Jasaitis, M.I. Verkhovsky, J.E. Morgan, M.L. Verkhovskaya, M. Wikström, Assignment and charge translocation stoichiometries of the major electrogenic phases in the reaction of cytochrome *c* oxidase with dioxygen, Biochemistry 38 (1999) 2697–2706.
[29] J.L. Rigaud, B. Pitard, D. Levy, Reconstitution of membrane proteins into liposomes: application to energy-transducing membrane proteins, Biochim. Biophys. Acta 1231 (1995) 223–246.
[30] P. Nicholls, V. Hildebrandt, J.M. Wrigglesworth, Orientation and reactivity of cytochrome aa3 heme groups in proteoliposomes, Arch. Biochem. Biophys. 204 (1980) 533–543.
[31] P. Rosen, I. Pecht, Conformational equilibria accompanying the electron transfer between cytochrome *c* (P551) and azurin from *Pseudomonas aeruginosa*, Biochemistry 15 (1976) 775–786.
[32] L.A. Drachev, A.A. Jasaitis, A.D. Kaulen, A.A. Kondrashin, E.A. Liberman, I.B. Nemecek, S.A. Ostroumov, A. Semenov, V.P. Skulachev, Direct measurement of electric current generation by cytochrome oxidase, H+-ATPase and bacteriorhodopsin, Nature 249 (1974) 321–324.
[33] M.I. Verkhovsky, J.E. Morgan, M.L. Verkhovskaya, M. Wikström, Translocation of electrical charge during a single turnover of cytochrome-c oxidase, Biochim. Biophys. Acta 1318 (1997) 6–10.
[34] J. Hendriks, NO in bacterial respiration, thesis, EMBL, Heidelberg (2000).
[35] M. Brändén, H. Sigurdson, A. Namslauer, R.B. Gennis, P. Ädelroth, P. Brzezinski, On the role of the K-proton transfer pathway in cytochrome *c* oxidase, Proc. Natl. Acad. Sci. U. S. A. 98 (2001) 5013–5018.
[36] J.O. Lagerstedt, J.C. Voss, Å. Wieslander, B.L. Persson, Structural modeling of dual-affinity purified Pho84 phosphate transporter, FEBS Lett. 578 (2004) 262–268.
[37] K. Ginalski, A. Elofsson, D. Fischer, L. Rychlewski, 3D-Jury: a simple approach to improve protein structure predictions, Bioinformatics 19 (2003) 1015–1018.
[38] A. Sali, T.L. Blundell, Comparative protein modelling by satisfaction of spatial restraints, J. Mol. Biol. 234 (1993) 779–815.
[39] W. Humphrey, A. Dalke, K. Schulten, VMD: visual molecular dynamics, J. Mol. Graph. 14 (1996) 33–38.
[40] A. Onufriev, D. Bashford, D.A. Case, Exploring protein native states and large-scale conformational changes with a modified generalized born model, Proteins 55 (2004) 383–394.
[41] L. Zhang, J. Hermans, Hydrophilicity of cavities in proteins, Proteins 24 (1996) 433–438.

[42] S. Subramaniam, The Biology Workbench—a seamless database and analysis environment for the biologist, Proteins 32 (1998) 1–2.
[43] J.D. Thompson, D.G. Higgins, T.J. Gibson, CLUSTAL W: improving the sensitivity of progressive multiple sequence alignment through sequence weighting, position-specific gap penalties and weight matrix choice, Nucleic Acids Res. 22 (1994) 4673–4680.
[44] M.I. Verkhovsky, A. Jasaitis, M.L. Verkhovskaya, J.E. Morgan, M. Wikström, Proton translocation by cytochrome *c* oxidase, Nature 400 (1999) 480–483.
[45] A. Kannt, H. Michel, M.R. Cheesman, A.J. Thomson, A.B. Dreusch, H. Körner, W.G. Zumft, The electron transfer centers of nitric oxide reductase: Homology with the heme-copper oxidase family, in: G. Canters, W. Vijgenboom (Eds.), Biological electron-transfer chains: genetics, composition and mode of operation, Kluwer Academic Publishers, Dordrecht, 1998, pp. 279–291.
[46] J. Hendriks, U. Gohlke, M. Saraste, From NO to OO: Nitric oxide and dioxygen in bacterial respiration, J. Bioenerg. Biomembr. 30 (1998) 15–24.
[47] F.H. Thorndycroft, G. Butland, D.J. Richardson, N.J. Watmough, A new assay for nitric oxide reductase reveals two conserved glutamate residues form the entrance to a proton-conducting channel in the bacterial enzyme, Biochem. J. 401 (2007) 111–119.
[48] D.M. Mitchell, J.R. Fetter, D.A. Mills, P. Ädelroth, M.A. Pressler, Y. Kim, R. Aasa, P. Brzezinski, B.G. Malmström, J.O. Alben, G.T. Babcock, S. Ferguson-Miller, R.B. Gennis, Site-directed mutagenesis of residues lining a putative proton transfer pathway in cytochrome *c* oxidase from *Rhodobacter sphaeroides*, Biochemistry 35 (1996) 13089–13093.
[49] U. Pfitzner, K. Hoffmeier, A. Harrenga, A. Kannt, H. Michel, E. Bamberg, O.M. Richter, B. Ludwig, Tracing the D-pathway in reconstituted site-directed mutants of cytochrome *c* oxidase from *Paracoccus denitrificans*, Biochemistry 39 (2000) 6756–6762.
[50] A. Namslauer, H. Lepp, M. Brändén, A. Jasaitis, M.I. Verkhovsky, P. Brzezinski, Plasticity of proton pathway structure and water coordination in cytochrome c oxidase, J. Biol. Chem. (in press) doi:10.1074/jbc.M700348200.
[51] R. Pomès, G. Hummer, M. Wikström, Structure and dynamics of a proton shuttle in cytochrome *c* oxidase, Biochim. Biophys. Acta 1365 (1998) 255–260.
[52] P. Ädelroth, M.S. Ek, D.M. Mitchell, R.B. Gennis, P. Brzezinski, Glutamate 286 in cytochrome aa3 from *Rhodobacter sphaeroides* is involved in proton uptake during the reaction of the fully-reduced enzyme with dioxygen, Biochemistry 36 (1997) 13824–13829.
[53] M.L. Verkhovskaya, A. Garcia-Horsman, A. Puustinen, J.L. Rigaud, J.E. Morgan, M.I. Verkhovsky, M. Wikström, Glutamic acid 286 in subunit I of cytochrome bo3 is involved in proton translocation, Proc. Natl. Acad. Sci. U. S. A. 94 (1997) 10128–10131.
[54] N.J. Watmough, A. Katsonouri, R.H. Little, J.P. Osborne, E. Furlong-Nickels, R.B. Gennis, T. Brittain, C. Greenwood, A conserved glutamic acid in helix VI of cytochrome bo3 influences a key step in oxygen reduction, Biochemistry 36 (1997) 13736–13742.
[55] M. Svensson-Ek, J.W. Thomas, R.B. Gennis, T. Nilsson, P. Brzezinski, Kinetics of electron and proton transfer during the reaction of wild type and helix VI mutants of cytochrome bo3 with oxygen, Biochemistry 35 (1996) 13673–13680.
[56] P. Ädelroth, M. Karpefors, G. Gilderson, F.L. Tomson, R.B. Gennis, P. Brzezinski, Proton transfer from glutamate 286 determines the transition rates between oxygen intermediates in cytochrome *c* oxidase, Biochim. Biophys. Acta, Bioenerg. 1459 (2000) 533–539.
[57] J. Goretski, O.C. Zafiriou, T.C. Hollocher, Steady-state nitric oxide concentrations during denitrification, J. Biol. Chem. 265 (1990) 11535–11538.
[58] L.M. Blomberg, M.R. Blomberg, P.E. Siegbahn, A theoretical study on nitric oxide reductase activity in a ba(3)-type heme-copper oxidase, Biochim. Biophys. Acta 1757 (2006) 31–46.
[59] A. Namslauer, A. Aagaard, A. Katsonouri, P. Brzezinski, Intramolecular proton-transfer reactions in a membrane-bound proton pump: the effect of pH on the peroxy to ferryl transition in cytochrome *c* oxidase, Biochemistry 42 (2003) 1488–1498.